Experimental test of the Rayleigh–Debye–Gans theory for light scattering by fractal aggregates

Genmiao Wang and Christopher M. Sorensen

Calibrated measurements of optical (λ = 488-nm) scattering cross sections, in the form of Rayleigh ratios, are presented for two fractal aggregate aerosols. The aggregates have radii of gyration of approximately 280 nm, fractal dimensions of approximately 1.75, and monomer sizes of approximately 20 nm with approximately 150 monomers per cluster. One aerosol was composed of vitreous SiO_2 with a refractive index of 1.46, the other of anatase TiO_2 with a refractive index of 2.61. We found good agreement with the Rayleigh–Debye–Gans prediction for the scattering cross section of fractal aggregates.

OCIS codes: 290.5870, 290.0290, 120.5820.

1. Introduction

Aggregates, found in both colloids and aerosols, abound in nature. It appears that, without exception, when solid particles come together by aggregation processes, the resulting random aggregates have a fractal morphology.[1,2] Even when other processes, such as sintering, occur as well, the resulting morphology is often adequately described as fractal. A fundamental relation to describe a fractal aggregate of N monomers (or primary particles) is

$$N = k_o(R_g/a)^D, \tag{1}$$

where k_o is a constant of order unity, R_g is the cluster radius of gyration (a root-mean-square radius), a is the monomer radius, and D is the fractal dimension. The key parameter for fractal description is the fractal dimension. The value of D is less than the spatial dimension, and this quantifies the openness of the cluster aggregate.

A considerable amount of research has been applied toward understanding the physical properties of aggregates. The topic of this paper is the optical light-scattering properties of fractal aggregates. This is important in a number of areas such as environmental applications involving visibility and radiation transfer and for optical diagnostics of aerosols and colloids.[3] Calculation of the optical properties by use of exact electromagnetic theory can be achieved with modern computational technology, but the problem is complex, computationally intensive, and gives little physical insight. As scientists, we look for simpler formulations with sufficient accuracy.

A simple formulation exists for optical scattering by aggregates in what has become known as the Rayleigh–Debye–Gans (RDG) formulation for fractal aggregates. However, the success or failure of this formulation is not tied to the fractal nature of the aggregate, rather it depends on the relative strength of intra-aggregate multiple scattering. This formulation originates from small-angle x-ray scattering[4–7] and small-angle neutron scattering[8] studies of fractal aggregates. The refractive index of materials for x rays is essentially unity, hence the scattering is simply the square of the Fourier transform of the real-space structure. Early light-scattering studies[4] of fractal aggregates in colloids employed a similar formulation. Berry and Percival[9] were the first to consider fractal aggregate optics, scattering, and absorption theoretically, and their results supported, for the most part, this simple procedure. The term Rayleigh–Debye–Gans is appropriate[10] because RDG theory for spherical particles holds when there is no internal multiple scattering, i.e., each subvolume of the object sees only the incident wave. This occurs when the phase-shift parameter ρ obeys[11,12]

$$\rho = 2kR|m - 1| < 1, \tag{2}$$

The authors are with the Department of Physics and Program for Complex Fluid Flows, Kansas State University, Manhattan, Kansas 66506-2601. C. M. Sorensen's e-mail address is sor@phys.ksu.edu.

Received 13 June 2001; revised manuscript received 19 April 2002.

0003-6935/02/224645-07$15.00/0

where $k = 2\pi/\lambda$ is the wave number for wavelength λ, R is the sphere radius, and m is the index of refraction of the sphere, possibly complex, relative to the medium. When Eq. (2) holds, the scattering cross section is simply the Fourier transform of the structure squared.

Previous tests of the RDG predictions have included both theoretical and experimental studies. These studies have been recently reviewed by one of us.[3] The earliest studies of the optics of fractal aggregates of Berry and Percival[9] followed by Nelson[13] assumed that the multiple scattering was uniform throughout the cluster, a mean-field approximation. For $D < 2$, they found that multiple scattering was not significant; this implies that RDG can be used in these cases. A number of subsequent studies concluded that RDG must be corrected upwards by 10–20% for $D < 2$ when $ka \leq 0.4$ and a real refractive index.[14–25] Recently Farias *et al.*[26] compared the exact volume integral effective field formulation of the electromagnetic scattering problem with RDG over a broad range of monomer refractive indices and size parameters ka. Our analysis[3] of their results showed that, when the aggregate's phase-shift parameter was less than approximately three, i.e.,

$$\rho^{\mathrm{agg}} = 2kR_g|m - 1| \leq 3, \tag{3}$$

the difference between the volume integral effective field and RDG was 10% or less. We concluded that ρ^{agg} was the key parameter.

Experimental tests of RDG cross sections have been indirect.[27,28] They have involved soot aerosols in flames. Experimentally measured cross sections were not compared with theory, but the RDG theory has been used to interpret light-scattering data to determine cluster parameters. Cluster parameters most sensitive to the cross sections are N and a. Comparison of N and a measured by light scattering interpreted with RDG to electron microscope measurements have been good, but the procedure is fraught with many errors. Sampling is perturbative, and transverse electron microscopy analysis involves two-dimensional projections of three-dimensional aggregates. Light scattering involves high moments of the size distribution, hence the measured distribution by transverse electron microscopy must be accurate to make comparisons. Furthermore, the refractive index of soot is poorly known.

In this paper we make a direct comparison of RDG-predicted scattering cross sections and those that are measured. We used aerosols of SiO_2 and TiO_2, which form fractal aggregates by diffusion-limited cluster aggregation[2] with $D \simeq 1.75$. The monomers have a size parameter of $ka = 0.26$ and a real refractive index. The absolute scattering from these aerosols was determined by calibration against liquids of known scattering power. Other data including aerosol mass density, monomer size, and refractive index are combined to compare the experimental with the RDG theory. Despite some limitations, we demonstrate the value of the RDG formulation.

2. Rayleigh–Debye–Gans Theory for Aggregate Scattering

We consider the usual experimental situation in which the incident light is vertically polarized, perpendicular to the horizontal scattering plane that contains the scattering angle. Under the RDG formulation, the scattering and absorption of an aggregate, not necessarily fractal, are given by the following cross sections.[3,29] For scattering, the differential scattering cross section is

$$\frac{d\sigma^{\mathrm{agg}}}{d\Omega} = N^2 \frac{d\sigma^m}{d\Omega} S(qR_g). \tag{4}$$

For absorption, it is

$$\sigma^{\mathrm{agg}} = N\sigma^m. \tag{5}$$

In Eqs. (4) and (5) the superscripts refer to aggregates and monomers. In Eq. (4) $S(qR_g)$ is the static structure factor of the aggregate, which is the $q = 0$ normalized square of the Fourier transform of the structure. The parameter q, given by

$$q = 4\pi\lambda^{-1} \sin(\theta/2), \tag{6}$$

is the scattering wave-vector magnitude at scattering angle θ. In this paper we use particles of SiO_2 and TiO_2 that have real refractive indices in the visible regime; hence they do not absorb. In this paper we do not consider absorption.

We use the form $d\sigma/d\Omega$ to stress that this is a differential cross section (square centimeter) per unit solid angle (steradian). We take the monomers as Rayleigh scatterers, i.e., $ka = 2\pi a/\lambda < 1$. Thus[11,12]

$$\frac{d\sigma^m}{d\Omega} = k^4 a^6 \left| \frac{m^2 - 1}{m^2 + 2} \right|^2. \tag{7}$$

The particles used here have radii of approximately $a = 20$ nm. With our experimental wavelength of $\lambda = 488$ nm (see Section 3), the size parameter is $ka = 0.26$, sufficiently small to be in the Rayleigh regime. Thus use of Eq. (7) is justified. It is the combination of Eqs. (4) and (7) that we test in this paper.

3. Experimental Methods

A. Aerosol Production

Both TiO_2 and SiO_2 aerosols were generated by thermal decomposition of either titanium tetraisopropoxide or tetraethyl orthosilicate, similar to the method reported by Okuyama *et al.*[30] We generated vapors by heating liquid titanium tetraisopropoxide or tetraethyl orthosilicate to temperatures around 80 °C and 30 °C, respectively, and then these vapors were carried into a half-meter-long tube furnace by dry N_2 gas with a flow rate of 0.5 l/min. The furnace

Table 1. Aerosol Physical Parameters

Material	Particle Density, ρ_p (g/cm^3)	Aerosol Density (10^{-6} g/cm^3)	Particle Average Refractive Index at λ = 488 nm	a_0 (nm)	σ	D	R_g (nm)
SiO_2	2.20	0.55 ± 0.06	1.463	20	1.15	1.78 ± 0.08	270 ± 20
TiO_2	3.84	1.0 ± 0.15	2.61	17	1.24	1.71 ± 0.08	280 ± 20

was set to a temperature of ~400 °C or ~900 °C, respectively. The vapors decomposed inside the furnace to form particles and were carried out of the furnace as an aerosol.

Transmission electron micrographs of the aggregates collected at the position of the optical scattering volume (see Section 4) showed aggregates composed of approximately spherical primary particles. For the TiO_2 aerosols, the measured radius of these monomers was $a = 17 \pm 4$ nm, where the quoted errors represent one standard deviation. X-ray diffraction showed the TiO_2 to have the anatase structure that has a density of $\rho = 3.84$ g/cm^3.[31]

The refractive indices of birefringent anatase are given in the literature for a wavelength of $\lambda = 589$ nm, the sodium D line, as 2.554 and 2.493.[31] We were unable to find data for other wavelengths. Because our scattering experiments were performed at $\lambda = 488$ nm, we have to make an estimate of the refractive index at this wavelength on the basis of the estimated dispersion and the known $\lambda = 589$-nm values. Moreover, because we are scattering from randomly oriented particles, we must start with an average of the two birefringent values. To perform this average we weighted the 2.554 value twice as much as the 2.493 value because it applies to two of the three crystal directions. This yields an average of $\langle m \rangle = 2.543$. An estimate of dispersion was gleaned from the behaviors of flint glasses in the region of $\lambda = 500$ nm.[31] It was found that dispersion increased with refractive index, and an extrapolation to $m \simeq 2.5$ was necessary because the largest refractive indices for these glasses was approximately 1.9. This led to a dispersion of $dm/d\lambda = 7.5 \times 10^{-4}$ nm^{-1} for anatase. From this we find $\langle m(488\text{ nm}) \rangle = 2.61$ for anatase. We used this value in our calculations.

For the SiO_2 aerosols, transverse electron micrographs showed the monomer radius to be $a = 20 \pm 3$ nm. The SiO_2 produced was shown by x-ray diffraction to be amorphous. It has a density of 2.20 g/cm^3 and a refractive index of 1.463 at $\lambda = 486$ nm.[31]

We measured the mass density of the aerosol by collecting the aerosol immediately after it left the orifice of the glass tube. Collection was achieved with a cylindrical cross-sectional funnel inverted and placed with its circular filter approximately 1 cm above the orifice. The exit side of the funnel was connected to a vacuum pump to draw the aerosol directly from the orifice to the filter. Visual inspection of the strongly scattering aerosol verified that no aerosol escaped or passed through the filter. Given the volumetric flow rate of aerosol measured with a flowmeter, elapsed collection time, and the mass of the collected aerosol powder, the aerosol mass density was determined. The aerosol physical parameters are listed in Table 1.

B. Light Scattering

The aerosol from the tube furnace passed vertically out from a circular 0.4-cm-diameter orifice with laminar flow into the room air. A few millimeters above this orifice the focused beam of an argon-ion laser with wavelength $\lambda = 488$ nm and vertical polarization passed through the flow. Scattered light from the aerosol was collected at a variety of scattering angles by a moveable photomultiplier tube. The signal from this photomultiplier tube was used as a measure of the scattered intensity. From this the static structure factors $S(q)$ shown in Fig. 1 were determined. The linearity of the large q regions of these plots indicates that the aggregates can be described by the fractal concept. The slopes yield the aggregate fractal dimension,[3,29] which we found to be $D = 1.71 \pm 0.08$ and 1.78 ± 0.08 for the TiO_2 and SiO_2 aerosols, respectively. Guinier analysis[3,29] of the curvature regimes of these graphs yielded the cluster radius of gyration, which was found to be 280 ± 20 and 270 ± 20 nm, respectively.

Absolute scattered intensity measurements were achieved by calibration of the aerosol scattering against scattering from liquids with a known Rayleigh ratio[11] (also known as Rayleigh factors) (see Table 2). Each calibration liquid was of high purity. They were contained in glass cylinders 2.5 cm in

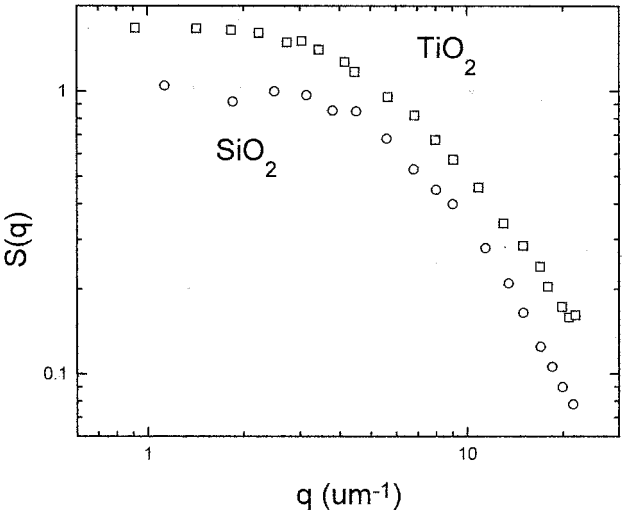

Fig. 1. Static structure factors $S(q)$ for SiO_2 (circles) and TiO_2 (squares) aerosols. $S(q)$ for TiO_2 was multiplied by 5/3.

Table 2. Rayleigh Ratios at λ = 488 nm and a Scattering Angle of 90° (R_v) and Index of Refraction for the Liquids Used

Liquid	R_v (10^{-6} cm^{-1} sr^{-1})	Refractive Index (m)
Carbon tetrachloride	17	1.47
Benzene	37	1.51
Toluene	41	1.51
Carbon disulphide	170	1.65

diameter that were filled and sealed under nitrogen. For calibration, the liquid cells were placed in the incident beam replacing the aerosol.

The scattering geometry for our experiments was one in which the incident light was polarized vertically (perpendicular to the scattering plane), but detection of the light did not use a polarizer. The scattering angle for calibration was $\theta = 90°$. Following the notation of Moreels *et al.*,[32] a Rayleigh ratio measured under these conditions is denoted by R_v. To obtain R_v we used data from Coumou *et al.*[33] for R_u, the Rayleigh ratio for unpolarized incident and detected light and ρ_u the depolarization ratio for unpolarized incident light both at $\lambda = 546$ nm. R_v is given by[32]

$$R_v = 2R_u/(1 + \rho_u). \tag{8}$$

The problem now is how to convert R_v values from $\lambda = 546$ to the 488 nm used here. We explored this empirically with a variety of Rayleigh ratio data[11,32,33] and found that the functionality λ^{-4}, the Rayleigh law, does not work. Instead, we found, to a good approximation,

$$R_v \sim \lambda^{-4.6\pm0.15}. \tag{9}$$

With this, we converted R_v to $\lambda = 488$ nm, and the results are given in Table 2. We remark that, in previous research,[34] we used the same four liquids but for R_{vv} values, i.e., vertical incident and vertical detected polarization. It can be shown that $R_v = 2R_{vv}/(2 - \rho_u)$, and this relation holds well at $\lambda = 488$ nm for the R_v values in Table 2 and the R_{vv} values in our previous research.

The scattered intensity for the liquids is given by

$$I = clI_{0v}R_v, \tag{10}$$

where I is the scattered intensity, I_{0v} is the intensity of the incident light vertically polarized, c is the calibration constant, and l is the length of the scattering volume, i.e., the detected length of the incident beam crossing the liquid or aerosol.

Refraction that is due to the cylindrical shape of the container containing the calibration liquids causes two effects. First, the incident beam refracts upon entering the cell, and this changes the cross-sectional width of the scattering volume. However, this does not affect calibration because the relevant incident quantity is the power, not the intensity. Second, the length of the scattering volume l detected by our apparatus will change because of refraction of the scattered light. Our apparatus collects the scattered light at a 90° scattering angle and images the scattering volume onto an iris. This determines the length of the observed scattering volume. With simple ray optics, one can show that the cylindrical container acts as a lens magnifying the length of the scattering volume by a factor equal to the refractive index of the liquid m. There is no such lensing effect with the aerosol. Thus a correction for m, of magnitude of approximately 1.5 (see Table 2), must be made. To do this we write the observed length as $l = l_0/m$ where l_0 is the length of the scattering volume when $m = 1.0$, e.g., in the aerosol. With this, Eq. (10) becomes

$$I = cI_{0v}l_0(R_v/m). \tag{11}$$

Thus, in our scattering geometry, a plot of scattered intensity versus R_v/m should be linear, and this is indeed true as shown in Fig. 2. To determine the Rayleigh ratio of an aerosol, we merely measure its scattered intensity I under the same conditions as Fig. 2 was created and find to what value of R_v/m, with $m = 1.0$, this corresponds to. These experimental aerosol Rayleigh ratios are given in Table 3.

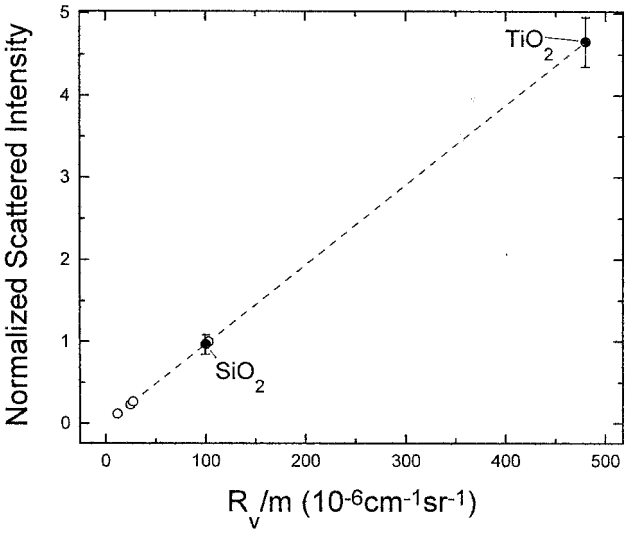

Fig. 2. Scattered intensities, normalized to the value obtained from CCl_4 versus the Rayleigh ratio divided by the medium refractive index. Open circles are the four liquids listed in Table 2; filled circles are the two aerosols listed in Table 3. Errors for the liquid scattered intensities are represented by the symbol size.

4. Scattering Analysis

The monomers in our experiments here have a size parameter no greater than $ka = 0.26$. For such a

Table 3. Comparison of Theoretically Expected Measured Rayleigh Ratios (10^{-6} cm^{-1} sr^{-1}) for the Two Aerosols

Material	ρ^{agg}	R_v (theory)	R_v (measured)
SiO_2	3.0	87 ± 20	100 ± 10
TiO_2	11	460 ± 150	480 ± 30

situation the exact Mie theory would predict an anisotropy in scattering between forward- and backward-angle scattering of only 1.3%. Thus we take our monomers as Rayleigh scatterers for which Eq. (7) holds.

The absolute scattering measurements made here rely on calibration against liquids with known Rayleigh ratios. Thus we consider the scattering Rayleigh ratio for a particulate system. When we let n be the particle number density, then the Rayleigh ratio is given in general by

$$R_v = n \frac{\mathrm{d}\sigma}{\mathrm{d}\Omega}. \tag{12}$$

The units of R_v are in $\mathrm{sr}^{-1}\ \mathrm{cm}^{-1}$.

To proceed further we must account for the size polydispersity of the clusters, which comes in two types. There is a polydispersity in monomer size and a polydispersity in cluster size. Then when we substitute Eq. (7) into Eq. (4) and add the result into Eq. (12), it leads to the scattering Rayleigh ratio

$$R_v = k^4 \left| \frac{m^2 - 1}{m^2 + 2} \right|^2 \iint p(a) n(N) a^6 N^2 S(qR_g) \mathrm{d}a \, \mathrm{d}N, \tag{13}$$

where $p(a)$ is the size distribution of monomers, based on the monomer radius a, and $n(N)$ is the cluster size distribution, number of clusters per unit volume based on the number of monomers per cluster N.

The scattering measurements were performed at $\theta = 90°$, hence $q = 18.2\ \mu\mathrm{m}^{-1}$. Both aerosols had $R_g = 280$ nm (nearly), thus $qR_g = 5.1$. In this range the single cluster structure factor is well described by[35]

$$S(qR_g) = C(qR_g)^{-D} \tag{14a}$$

$$= C(aq)^{-D} k_0 N^{-1}, \tag{14b}$$

where $C \simeq 1.0$. To obtain Eq. (14b) from Eq. (14a), Eq. (1) was used. Substitution of Eq. (14b) into Eq. (13) yields for the Rayleigh ratio

$$R_v = k_0 C q^{-D} k^4 \left| \frac{m^2 - 1}{m^2 + 2} \right|^2 \int p(a) a^{6-D} \mathrm{d}a \int n(N) N \mathrm{d}N. \tag{15}$$

We determined the distribution $p(a)$ for the monomer radius by measuring numerous monomer radii on transverse electron micrographs of samples taken from the scattering volume region of the aerosol. As described above, $a = 17 \pm 4$ and 20 ± 3 nm for TiO_2 and SiO_2 aerosols, respectively, where the quoted uncertainties are the geometric standard deviations of the zeroth-order log-normal distribution, which does an adequate job of describing the distribution. The zeroth-order log-normal distribution is given by

$$p(a) = p_0 \exp[-ln^2(a/a_0)/2ln^2\sigma], \tag{16}$$

where p_0 is a normalization constant. We define the ith moment as

$$M_i = \int a^i p(a) \mathrm{d}a \tag{17}$$

and find

$$M_i = p_0 \exp[0.5(i + 1)^2 ln^2\sigma], \tag{18}$$

which is used below.

The cluster size distribution does not need to be known because it occurs in the aerosol mass density measurement as well as the Rayleigh ratio, and a cancellation occurs. To see this, realize that the aerosol mass density is given by the product of the monomer particle mass density ρ_p, the volume of each particle $4\pi a^3/3$, and the total number of monomers per unit volume nN, where n is the cluster number density. For a polydisperse situation, n is a function of N and this yields

$$\rho_{\mathrm{aero}} = \rho_p (4\pi/3) \int p(a) a^3 \mathrm{d}a \int n(N) N \mathrm{d}N. \tag{19}$$

The last integral in Eq. (19) is also found in Eq. (15) for the Rayleigh ratio. Substitution on this integral from Eq. (19) into Eq. (15) yields an expression independent of $n(N)$. The resulting expression involves a ratio of the moments of $p(a)$, Eq. (17), the $i = 6 - D$ moment divided by the $i = 3$ moment. This ratio can be evaluated with Eq. (18). The final expression is

$$R_v = k_0 C q^{-D} (3/4\pi)(\rho_{\mathrm{aero}}/\rho_p) {a_0}^{3-D} k^4 \left| \frac{m^2 - 1}{m^2 + 2} \right|^2 \times \exp[0.5(33 - 14D + D^2) ln^2\sigma]. \tag{20}$$

With Eq. (20) we calculate the expected (or theoretical) value of the Rayleigh ratio and compare it with the measured value. The input parameters to Eq. (20) and their uncertainties are now addressed.

The value of k_0 has been somewhat controversial.[3] Research from this laboratory has consistently found[36–38]

$$k_0 = 1.3 \pm 0.1$$

for diffusion-limited cluster aggregation aggregates with $D_f \simeq 1.75$.

The value of C depends on the nature of the cutoff of the density at the perimeter of the aggregate. For diffusion-limited cluster aggration, we established aggregates with $D \simeq 1.75$[35]:

$$C = 1.0 \pm 0.1.$$

The value of q at $\theta = 90°$ for $\lambda = 488$ nm is $18.2\ \mu\mathrm{m}^{-1}$.

Structure factor measurements of Fig. 1 find the fractal dimensions and uncertainties given in Table 1.

The mass densities of the two aerosols were measured as described above with uncertainties of the

order of 10–15%. Other relevant quantities for the aerosols are listed in Table 1.

The refractive index for vitreous SiO_2 is well determined. On the other hand, averaging and estimates of dispersion were necessary to find $m = 2.61$ for anatase at $\lambda = 488$ nm. Use of the $\lambda = 589$-nm average value of $m = 2.543$ would cause the Lorentz factor of Eq. (20), namely, $|(m^2 - 1)/(m^2 + 2)|^2$, to be 4.3% smaller. This implies that the uncertainty that is due to the refractive index is small, less than 4%.

All these quantities can now be put into Eq. (20) to calculate the theoretical (expected) value of the Rayleigh ratio for the aerosols. The uncertainties in all the input parameters were used to determine the uncertainty of the R_v value. These are compared with the measured values in Table 3, which also includes the phase-shift parameter for the two clusters ρ^{agg}.

5. Conclusion

The agreement between theory and experiment is quite good, well within the uncertainties. The theoretical uncertainties are large (~20–30%) because of significant uncertainties in the parameters that go into Eq. (20) for the Rayleigh ratio. In fact we confess some degree of surprise at the good agreement given the large number of parameters, all with some degree of uncertainty, that are involved in both the theoretical and the experimental determinations of the Rayleigh ratio. Our previous analysis[3] summarized in Eq. (3) implied that good agreement should occur for the SiO_2 aerosol that has an aggregate phase-shift parameter of 3.0. However, for TiO_2, the aggregate phase-shift parameter ρ^{agg} is equal to 11, which is well beyond the criterion of Eq. (3), namely, $\rho^{agg} \leq 3$, the region in which RDG is expected to be accurate. Thus we look for a closer comparison to the results of Farias *et al.*,[26] which Eq. (3) tries to summarize. To do so, we first calculate the number of monomers from Eq. (1), $k_0 = 1.3$ and the R_g, a, and D values of Table 1. We find $N = 190$. We also have $ka = 0.22$ and $m = 2.61$. Farias *et al.* plot contours of the deviation of RDG theory and the exact electromagnetic result on graphs with ka and $m - 1$ as axes for values of N up to 256. When we plot our aerosol on their results (Fig. 2 of their paper), we find a prediction of approximately a 10% error. The error is small because, as explained by Farias *et al.*, two major non-RDG effects are nearly canceling in this region of the $(m - 1)$ versus ka plot to bring the electromagnetic result close to the RDG prediction. Regardless of the reason for the error, our experimental results, limited as they are, are consistent with their predictions.

This research was supported by National Science Foundation grants CTS 9709764 and CTS0080017.

References

1. S. R. Forrest and T. A. Witten, Jr., "Long-range correlations in smoke-particle aggregates," J. Phys. A **12,** L109–L117 (1979).
2. R. Jullien and R. Botet, *Aggregation and Fractal Aggregates* (World Scientific, Singapore, 1987).
3. C. M. Sorensen, "Light scattering by fractal aggregates. A review," Aerosol Sci. Technol. **35,** 648–687 (2001).
4. D. W. Schaefer, J. E. Martin, P. Wiltzius, and D. S. Cannell, "Fractal geometry of colloidal aggregates," Phys. Rev. Lett. **52,** 2371–2374 (1984).
5. J. E. Martin, D. W. Schaefer, and A. J. Hurd, "Fractal geometry of vapor-phase aggregates," Phys. Rev. A **33,** 3540–3543 (1986).
6. J. Teixeira, "Experimental methods for studying fractal aggregates," in *On Growth and Form, Fractal and Non-Fractal Patterns in Physics*, H. E. Stanley and N. Ostrowski, eds. (Nijhoff, Dordrecht, The Netherlands, 1986) pp. 145–165.
7. J. E. Martin and A. J. Hurd, "Scattering from fractals," J. Appl. Crystallogr. **20,** 61–78 (1987).
8. T. Freltoft, J. K. Kjems, and S. K. Sinha, "Power-law correlations and finite-size effects in silica particle aggregates studied by small-angle neutron scattering," Phys. Rev. B **33,** 269–272 (1986).
9. M. V. Berry and I. C. Percival, "Optics of fractal clusters such as smoke," Opt. Acta **33,** 577–591 (1986).
10. U. O. Köylü and G. M. Faeth, "Optical properties of overfire soot in buoyant turbulent diffusion flames at long residence times," J. Heat Transfer **116,** 152–159 (1994).
11. M. Kerker, *The Scattering of Light and Other Electromagnetic Radiation* (Academic, New York, 1969).
12. H. C. van de Hulst, *Light Scattering by Small Particles* (Wiley, New York, 1957).
13. J. Nelson, "Test of mean field theory for the optics of fractal clusters," J. Mod. Opt. **36,** 1031–1057 (1989).
14. J. Frey, J. J. Pinvidic, R. Botet, and R. Jullien, "Light scattering by fractal aggregates: a numerical investigation," J. Phys. (Paris) **49,** 1969–1976 (1988).
15. M. F. Iskander, H. Y. Chen, and J. E. Penner, "Optical scattering and absorption by branched chains of aerosols," Appl. Opt. **28,** 3083–3091 (1989).
16. A. R. Jones, "Electromagnetic wave scattering by assemblies of particles in the Rayleigh approximation," Proc. R. Soc. London Ser. A **366,** 111–127 (1979).
17. J. C. Ku, "Correction for the extinction efficiency factors given in the Jones solution for electromagnetic scattering by agglomerates of small spheres," J. Phys. D **24,** 71–75 (1991).
18. J. C. Ku and K.-H. Shim, "A comparison of solutions for light scattering and absorption by agglomerated or arbitrarily-shaped particles," J. Quant. Spectrosc. Radiat. Transfer **47,** 201–220 (1992).
19. W. Lou and T. T. Charalampopoulos, "On the electromagnetic scattering and absorption of agglomerated small spherical particles," J. Phys. D **27,** 2258–2270 (1994).
20. D. W. Mackowski, "Calculation of total cross sections of multiple-sphere clusters," J. Opt. Soc. Am. A **11,** 2851–2861 (1994).
21. D. W. Mackowski, "Electrostatic analysis of radiative absorption by sphere clusters in the Rayleigh limit: application to soot clusters," Appl. Opt. **34,** 3535–3545 (1995).
22. R. D. Mountain and G. W. Mulholland, "Light scattering from simulated smoke agglomerates," Langmuir **4,** 1321–1326 (1988).
23. G. W. Mulholland, C. F. Bohren, and K. A. Fuller, "Light scattering by agglomerates: coupled electric and magnetic dipole method," Langmuir **10,** 2533–2546 (1994).
24. J. Mullins and A. Williams, "The optical properties of soot: a comparison between experimental and theoretical values," Fuel **66,** 277–284 (1987).
25. S. B. Singham and C. F. Bohren, "Scattering of unpolarized and polarized light by particle aggregates of different size and fractal dimension," Langmuir **9,** 1431–1435 (1993).

26. T. L. Farias, U. O. Koylu, and M. G. Carvalho, "Range of validity of the Rayleigh–Debye–Gans theory for optics of fractal aggregates," Appl. Opt. **35,** 6560–6567 (1996).
27. J. Cai, N. Lu, and C. M. Sorensen, "Comparison of size and morphology of soot aggregates as determined by light scattering and electron microscope analysis," Langmuir **9,** 2861–2867 (1993).
28. U. O. Köylü, Y. Xing, and D. E. Rosner, "Fractal morphology analysis of combustion-generated aggregates using angular light scattering and electron microscope images," Langmuir **11,** 4848–4854 (1995).
29. C. M. Sorensen, "Scattering and absorption of light by particles and aggregates," in *Handbook of Surface and Colloid Chemistry*, K. S. Birdi, ed. (CRC Press, Boca Raton, Fla., 1997), pp. 533–558.
30. K. Okuyama, R. Ushio, Y. Kousaka, R. C. Flagan, and J. H. Seinfeld, "Particle generation in a chemical vapor deposition process and seed particles," AIChE J. **36,** 409–422 (1990).
31. R. C. Weast, ed., *Handbook of Chemistry and Physics* (CRC Press, Cleveland, Ohio, 1976), Vol. 51.
32. E. Moreels, W. De Ceuninck, and R. Finsy, "Measurements of the Rayleigh ratio of some pure liquids at several laser light wavelengths," J. Chem. Phys. **86,** 618–623 (1987).
33. D. J. Coumou, E. L. Mackor, and J. Hijmans, "Isotropic light-scattering in pure liquids," Trans. Faraday Soc. **60,** 1539–1547 (1964).
34. B. J. Olivier, C. M. Sorensen, and T. W. Taylor, "Scaling dynamics of aerosol coagulation," Phys. Rev. A **45,** 5614–5622 (1992).
35. C. M. Sorensen and G. M. Wang, "Size distribution effect on the power law regime of the structure factor of fractal aggregates," Phys. Rev. E **60,** 7143–7148 (1999).
36. J. Cai, N. Lu, and C. M. Sorensen, "Analysis of fractal cluster morphology parameters: structural coefficient and density autocorrelation function cutoff," J. Colloid Interface Sci. **171,** 470–473 (1995).
37. C. M. Sorensen and G. C. Roberts, "The prefactor of fractal aggregates," J. Colloid Interface Sci. **186,** 447–452 (1997).
38. C. Oh and C. M. Sorensen, "The effect of monomer overlap on the morphology of fractal aggregates," J. Colloid Interface Sci. **193,** 17–25 (1997).